

A Modification of CIECAM02 Based on the Hunt–Pointer–Estevez Matrix

Changjun Li

School of Electronics and Information Engineering, University of Science and Technology Liaoning, Anshan, 114051, China
 E-mail: cjli.cip@googlemail.com

M. Ronnier Luo[▲]

School of Design, University of Leeds, Leeds LS2 9JT, United Kingdom

Pei-Li Sun

Colour, Imaging & Illumination Centre, National Taiwan University of Science and Technology, Taipei, 10607, Taiwan

Abstract. This article describes modifications to the CIECAM02 appearance model based on the Hunt–Pointer–Estevez (HPE) matrix together with a revised nonlinear luminance adaptation function. The modified model removes the mathematical inconsistencies for both the forward and the inverse models that occur with CIECAM02 for highly saturated colors. The modified CIECAM02 can be considered an interim solution for use in color management for cross-media color reproduction before an updated version of CIECAM02 is developed by CIE Technical Committee. The modified model, however, performed 0.3 CV units worse than the original in predicting visual data derived by magnitude estimation, and an average of 1.3 CIELAB color difference units worse when predicting corresponding color data sets. © 2013 Society for Imaging Science and Technology.
 [DOI: 10.2352/J.ImagingSci.Technol.2013.57.3.030502]

INTRODUCTION

Since the recommendation of the CIECAM02 appearance model^{1,2} by CIE TC8-01, *Colour Appearance Modelling for Colour Management Systems*, it has been used to predict color appearance under a wide range of viewing conditions,^{1,2} to specify color appearance and evaluate image quality in terms of perceptual attributes,^{3–5} to quantify color differences,⁶ to provide a uniform color space⁷ and to provide a profile connection space for color management.^{8–10} However, many problems have been identified^{9–20} and various approaches have been proposed to modify the model to enable it to be used in all practical applications. There are two main problems. The first is the mathematical inconsistencies such as the lightness, J , computation given by

$$J = 100(A/A_w)^{cz}. \quad (1)$$

Throughout this article, the notations used are the same as those in the CIE Publication 159:2004¹; hence they have the

[▲] IS&T Member.

Received Jul. 13, 2012; accepted for publication Jul. 7, 2013; published online May 1, 2013. Associate Editor: Susan Farnand.
 1062-3701/2013/57(3)/030502/8/\$20.00

same meanings and thus

$$A = [2R'_a + G'_a + (1/20)B'_a - 0.305]N_{bb}. \quad (2)$$

A_w was shown to be positive²¹; A , however, can be negative. In this case, the ratio (A/A_w) in Eq. (1) is negative and raising a negative number to the power cz is mathematically undefined, which causes some unexpected computational failures.

The second problem is the instability problem which comes from the nonlinear post-luminance adaptation:

$$\begin{aligned} R'_a &= \frac{\text{sign}(R') * 400(F_L|R'|/100)^{0.42}}{27.13 + (F_L|R'|/100)^{0.42}} + 0.1 \\ G'_a &= \frac{\text{sign}(G') * 400(F_L|G'|/100)^{0.42}}{27.13 + (F_L|G'|/100)^{0.42}} + 0.1 \\ B'_a &= \frac{\text{sign}(B') * 400(F_L|B'|/100)^{0.42}}{27.13 + (F_L|B'|/100)^{0.42}} + 0.1. \end{aligned} \quad (3)$$

Here, the sign function, $\text{sign}(q)$, is 1 if $q > 0$, is -1 if $q < 0$ and is 0 if $q = 0$. The nonlinear function

$$f(q) = \frac{\text{sign}(q)400(F_L|q|/100)^{0.42}}{27.13 + (F_L|q|/100)^{0.42}} + 0.1 \quad (4)$$

has an infinite slope when $q = 0$, which causes instability^{11,13} for the inverse CIECAM02 model.

Note that both problems come mainly from the fact that R' , G' and B' can be very small, zero or negative. Let

$$p' = (R' \ G' \ B')^T, \quad g = (X \ Y \ Z)^T. \quad (5)$$

Here, superscript T is the transpose of a vector or matrix. Let M_{CAT02} and M_{HPE} be the CAT02 and Hunt–Pointer–Estevez (HPE) matrix^{1,2} respectively, and it can be shown that²⁰

$$p' = DM_{\text{HPE}}M_{\text{CAT02}}^{-1}\Lambda M_{\text{CAT02}}g + (1 - D)M_{\text{HPE}}g, \quad (6)$$

where D is the adaptation factor with a value between 0 and 1, and Λ is defined by

$$\Lambda = \begin{pmatrix} Y_w/R_w & & \\ & Y_w/G_w & \\ & & Y_w/B_w \end{pmatrix}. \quad (7)$$

Note that Eq. (7) will have a problem if the value of R_w , G_w or B_w is zero, which was noted first by Brill and Mahy.¹⁸ In fact, if, for example, a purple test illuminant is used or, more precisely, the test illuminant has chromaticity coordinates located on the $G = 0$ side of the CAT02 triangle,^{11,13} then G_w is indeed equal to 0.

Li et al.^{17,20} noted that if the CAT02 matrix is replaced by the HPE matrix, Eq. (6) becomes

$$p' = D\Lambda M_{\text{HPEG}} + (1 - D)M_{\text{HPEG}}. \quad (8)$$

Furthermore, they showed that if the value of g for the input sample (see Eq. (5)) has chromaticity coordinates inside the domain (denoted by Ω_{CMF} from now on) enclosed by the CIE spectral locus and the purple line, then

$$M_{\text{HPEG}} \geq 0. \quad (9)$$

Hence, p' in Eq. (8) is non-negative. In other words, R' , G' and B' are non-negative, which ensures that R'_a , G'_a and B'_a defined by Eq. (3) are not less than 0.1. Therefore, it follows that A defined by Eq. (2) is non-negative, which ensures that the lightness, J , defined by Eq. (1) is well defined.

Note that all the arguments above require the implicit assumption that the chromaticity coordinates of the test illuminant are located inside the domain Ω_{CMF} ; all real illuminants satisfy this assumption.

To correct the instability, the nonlinear function, f , defined by Eq. (4) must be updated. Gill¹⁶ considered linearizing the function at two ends. Let q_L and q_U be small and large positive constants respectively. For a value of q between the two constants, the function f is unchanged. When $q > q_U$, $f(q)$ is replaced by a linear function $f_{GU}(q)$ with $f_{GU}(q_U) = f(q_U)$ and the two functions have the same derivative at the point q_U , which ensures a continuous and smooth transition at that point. At the lower end $f(q)$ is replaced by a linear function $f_{GL}(q)$ for $q < q_L$ with $f_{GL}(q_L) = f(q_L)$ with the slope of the function being the difference ratio, an approximation to the derivative of the function $f(q)$ at $q = q_L$. Brill and Mahy¹⁸ also modified the function $f(q)$ slightly when $q > q_L$ and when $q < q_L$ the function is replaced by $f_{\text{BML}}(q)$. The functions $f_{\text{BML}}(q)$ and $f(q)$ have the same values and derivatives at $q = q_L$. Note that when q_L is small, the two functions $f_{\text{GL}}(q)$ and $f_{\text{BML}}(q)$ are similar. Thus, to repair the instability, the function $f(q)$ defined by Eq. (4) can be extended as $f_e(q)$ defined by the

following:

$$f_e(q) = \begin{cases} f(q_U) + \frac{df(q_U)}{dq}(q - q_U) & \text{if } q \geq q_U \\ f(q) & \text{if } q_L < q < q_U \\ f(q_L) + \frac{df(q_L)}{dq}(q - q_L) & \text{if } q \leq q_L. \end{cases} \quad (10)$$

Here, $df(q)/dq$ is the derivative of the function $f(q)$.

Note that Gill suggested that $q_L = 0.5$ and $q_U = 10^8$. The introduction of the linear function when $q > q_U$ enables the function $f_e(q)$ to be inverted.

From the above discussion, it can be seen that, if the CAT02 matrix is replaced by the HPE matrix, the mathematical inconsistencies have been overcome. In fact, the authors²⁰ have attempted to replace the CAT02 matrix with various matrices, including those proposed by Brill and Süsstrunk,^{11,13,18} Li et al.,^{14,17} and the HPE matrix, and tested the performance of the resulting models by predicting the experimental results from corresponding colors and color appearance data sets. However, all of these data sets, except for the HPE matrix, do not satisfy the nested rule^{13,18} among the non-negative response regions for the HPE matrix and the matrix for the CAT02 and the domain Ω_{CMF} . One motivation for this article was to investigate whether simplifying the CIECAM02 model by replacing the CAT02 matrix with the HPE matrix would better predict the experimental data when also including the above modifications.

In the next section, the modified model is presented, where there are three changes: the replacement of the CAT02 matrix by the HPE matrix, the replacement of the nonlinear function $f(q)$ by its extension $f_e(q)$ and a small change to the HPE matrix itself. With the modified version of the model, the mathematical inconsistencies and the instability for the forward and inverse CIECAM02 models are overcome. The inverse modified model is given in the Appendix; this has been implemented in MATLAB and its correctness further confirmed. The performance of the modified version is finally compared with the original version.

Note that Fairchild²² also evaluated different chromatic adaptation transforms using Munsell samples under different illuminants. He also included a version with the HPE matrix. Amongst all the transforms, the Fairchild optimized linear model,^{22,23} the Süsstrunk and Finlayson model,²⁴ the CMCCAT2000²⁵ and the modified CMC-CAT2000 transform^{2,22} performed much better than that based on the HPE matrix. However, Fairchild evaluated the performance of the models using only the Munsell data transformed under different illuminants, rather than the experimental corresponding datasets.²⁶ Finally, CIE TC8-01 made further tests and finally selected the CAT02 (modified CMCCAT2000)² to be used in CIECAM02.

The CIECAM02 model enjoys wide application in scientific research and industrial applications. However, computational problems were reported when the CIECAM02 model was used in color management for cross-media

color image reproduction, which led to the formation of CIE TC8-11 *CIECAM02-Mathematics* in 2007. In 2009 and 2012, Li et al.^{17,19} reported that the computational problems could be overcome and the resulting model would be simpler if the CAT02 matrix was replaced by the HPE matrix. However, the predictive accuracy would be poorer. Subsequently, the results of evaluation of a different modified version²⁰ were reported for prediction of the color appearance data sets based on magnitude estimation²⁷ and the corresponding colors.²⁵ This article systematically summarizes all the earlier publications and also adds new information on the inverse version to conclude the work on the modification of CIECAM02 based on a simple HPE model. The modifications to the current CIECAM02 model might be considered an interim solution for use in color management for cross-media color reproduction before an updated appearance model CIECAM02 is developed by the CIE Technical Committee.

A consensus has been achieved within TC8-11 to revise CIECAM02 using one simple matrix to combine the HPE and chromatic adaptation matrices. The revised version should predict more accurately than the HPE version without the mathematical inconsistency problem. For the majority of applications, which do not deal with imaging type over saturated data, the original CIECAM02 should still be used.

MODIFICATIONS TO CIECAM02

In this section, the modifications to the CIECAM02 model will be presented, which are the result of replacing the CAT02 matrix

$$M_{\text{CAT02}} = \begin{bmatrix} 0.7328 & 0.4296 & -0.1624 \\ -0.7036 & 1.6975 & 0.0061 \\ 0.0030 & 0.0136 & 0.9834 \end{bmatrix} \quad (11)$$

with the HPE matrix

$$M_{\text{HPE}} = \begin{bmatrix} 0.38971 & 0.68898 & -0.07869 \\ -0.22981 & 1.18340 & 0.04641 \\ 0.00000 & 0.00000 & 1.00000 \end{bmatrix}. \quad (12)$$

The modified version is simpler than the original CIECAM02 model and also overcomes the mathematical inconsistencies that existed with the original. In addition, the nonlinear luminance adaptation function $f(q)$ (Eq. (4)) is replaced by $f_e(q)$ defined by Eq. (10).

Note that the value -0.07869 in the HPE matrix at position (1, 3) is different from the HPE matrix^{1,2} in the original CIECAM02 model, where the value is -0.07868 . With the original, the sum of the first row is not equal to unity, which was pointed out by Kuo et al.^{9,10} They also gave a different solution by changing each of the elements in the first row.

Inputs and viewing conditions

The input data are the same as for the original CIECAM02 model:

- X_W, Y_W, Z_W : the tristimulus values of the test illuminant;
- L_A : the luminance of the test adapting field (in terms of cd/m^2);
- X_b, Y_b, Z_b : the tristimulus values of the background;
- X, Y, Z : the tristimulus values of the sample under the test illuminant;

and the viewing conditions are as follows:

Viewing conditions	c	N_c	F
Average surround	0.69	1.0	1.0
Dim surround	0.59	0.9	0.9
Dark surround	0.525	0.8	0.8

Step 0: All the parameters depending on the viewing conditions are computed using the following formulas:

$$k = 1/(5L_A + 1) \quad (13)$$

$$F_L = 0.2k^4(5L_A) + 0.1(1 - k^4)^2(5L_A)^{1/3} \quad (14)$$

$$n = Y_b/Y_W \quad (15)$$

$$N_{bb} = N_{cb} = 0.725(1/n)^{0.2} \quad (16)$$

$$z = 1.48 + \sqrt{n} \quad (17)$$

$$\begin{bmatrix} R_W \\ G_W \\ B_W \end{bmatrix} = \mathbf{M}_{\text{HPE}} \begin{bmatrix} X_W \\ Y_W \\ Z_W \end{bmatrix} \quad (18)$$

$$D = F \left[1 - \left(\frac{1}{3.6} \right) e^{\left(\frac{-(L_A+42)}{92} \right)} \right] \quad (19)$$

$$\Lambda_R = [(Y_w D/R_w) + (1 - D)]$$

$$\Lambda_G = [(Y_w D/G_w) + (1 - D)] \quad (20)$$

$$\Lambda_B = [(Y_w D/B_w) + (1 - D)]$$

$$R_{wc} = \Lambda_R R_w$$

$$G_{wc} = \Lambda_G G_w \quad (21)$$

$$B_{wc} = \Lambda_B B_w$$

$$R'_{aw} = f_e(R_{wc})$$

$$G'_{aw} = f_e(G_{wc}) \quad (22)$$

$$B'_{aw} = f_e(B_{wc})$$

$$A_w = [2R'_{wa} + G'_{wa} + (1/20)B'_{wa} - 0.305]N_{bb}. \quad (23)$$

Note 1: $R_w, G_w, B_w, D, \Lambda_R, \Lambda_G$ and Λ_B defined by Eqs. (18)–(20) are used to allow for chromatic adaptation. D is the adaptation factor and has a value between 0 and 1. If it is beyond the two boundaries it is set to the nearest boundary. Λ_R, Λ_G and Λ_B are weighted adaptation factors for the red, green and blue cone channels respectively. All the parameters computed from Eqs. (13)–(23) are input sample independent, i.e., in an image processing sense they are pixel

independent. Hence, they need only be computed once. The nonlinear luminance adaptation function $f_e(q)$ is defined by Eq. (10).

Note 2: Brill and Mahy¹⁸ noted that R_W , G_W or B_W in the chromatic adaptations (Eqs. (20)–(22)) may be zero for the original CIECAM02. However, with the new version, R_W , G_W and B_W will be positive if the chromaticity coordinates of the test illuminant are located inside the domain Ω_{CMF} .

Step 1: Chromatic Adaptation

Transform to cone space using the (modified) HPE matrix (12):

$$\begin{bmatrix} R \\ G \\ B \end{bmatrix} = \mathbf{M}_{\text{HPE}} \begin{bmatrix} X \\ Y \\ Z \end{bmatrix}. \quad (24)$$

Apply D factor weighted chromatic adaptation in cone space:

$$\begin{aligned} R_c &= \Lambda_R R \\ G_c &= \Lambda_G G \\ B_c &= \Lambda_B B. \end{aligned} \quad (25)$$

Note 3: the chromatic adaptation for the original CIECAM02 model is made in the ‘sharp sensor’ space since its spectral responses related to the CAT02 matrix (Eq. (11)) have negative values. On the other hand, in the current version of the CIECAM02 model with the (modified) HPE matrix, the tristimulus values X , Y , Z are transformed to cone space and chromatic adaptation is also applied in cone space.

Step 2: Allow for luminance adaptation by applying a nonlinear compression:

$$\begin{aligned} R'_a &= f_e(R_c) \\ G'_a &= f_e(G_c) \\ B'_a &= f_e(B_c). \end{aligned} \quad (26)$$

Here, the function $f_e(q)$ is given by Eq. (10).

Note 4: with the original CIECAM02 model the chromatic adaptation is made in the ‘sharp sensor’ space and thus, after adaptation, the adapted R_c , G_c and B_c values are transformed back to tristimulus values space by applying the inverse of the CAT02 matrix to R_c , G_c and B_c to calculate X_c , Y_c and Z_c . In order to carry out the luminance adaptation in cone space, the tristimulus values X_c , Y_c and Z_c are transformed to cone space by applying the HPE matrix to X_c , Y_c and Z_c to calculate R' , G' and B' . The luminance adaptation is completed by applying the nonlinear compressions $f(q)$ defined by Eq. (4) to R' , G' and B' . It can be seen that this is much simpler in the new version. As noted in note 3, R_c , G_c and B_c are in the cone space and are the chromatic adapted values. Hence the luminance adaptation is completed by applying the nonlinear compressions (Eq. (26)) directly to R_c , G_c and B_c . The new version is not only simpler, but also enjoys the nice

Table I. Unique hue data for the calculation of hue quadrature.

	Red	Yellow	Green	Blue	Red
i	1	2	3	4	5
h_i	20.14	90.00	164.25	237.53	380.14
e_i	0.8	0.7	1.0	1.2	0.8
H_i	0.0	100.0	200.0	300.0	400.0

property

$$R'_a \geq 0.1, \quad G'_a \geq 0.1, \quad B'_a \geq 0.1 \quad (27)$$

if the chromaticity coordinates of the input tristimulus values X , Y , Z are located inside or on the boundary of the domain Ω_{CMF} . It is because of this property that all mathematical inconsistencies with the CIECAM02 model are overcome, which will be discussed in the following steps.

Note 5: with the use of the extended function $f_e(q)$ for the luminance adaptation, the instability of the inverse model is overcome. In addition, for any real value β , $\beta = f_e(q)$ always has a unique solution for q .

Step 3: Transform to Opponent Color Space

Compute A or the achromatic response:

$$A = [2R'_a + G'_a + (1/20)B'_a - 0.305]N_{\text{bb}}. \quad (28)$$

Note 6: with the original CIECAM02 model, A may be negative. This causes the CIECAM02 model to have a computational problem when computing lightness, J . In the new version, however, A is non-negative as long as the chromaticity coordinates of the input tristimulus values X , Y , Z are located inside or on the boundary of the region Ω_{CMF} .

Calculate temporary Cartesian representations (a and b):

$$a = R'_a - 12G'_a/11 + B'_a/11 \quad (29)$$

$$b = (1/9)(R'_a + G'_a - 2B'_a). \quad (30)$$

Step 4: Compute Hue

Compute hue angle:

$$h = \tan^{-1}(b/a). \quad (31)$$

The hue angle, h , should be computed in degrees between 0° and 360° .

Hue quadrature, or H , can be computed from linear interpolation of the data shown in Table I using Eq. (32). If $h < h_1$, then $h' = h + 360$, otherwise $h' = h$. Choose a value of i so that $h_i \leq h' < h_{i+1}$.

$$H = H_i + \frac{100(h' - h_i)/e_i}{(h' - h_i)/e_i + (h_{i+1} - h')/e_{i+1}}. \quad (32)$$

Step 5: Predicting Perceptual Correlate Attributes

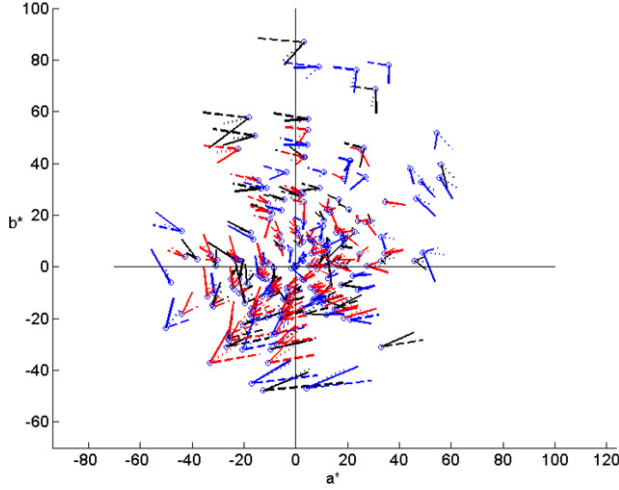


Figure 1. Color shifts for the Lam (blue lines), CSAJ (red lines) and Helson (black lines) datasets. The points with circles are the sample points under the test illuminant. The solid lines with open ends are the visual results under the reference illuminant; the dotted lines with open ends are the predictions using the original CAT02 matrix under the reference illuminant; the dashed lines are the predictions using the CAT02 matrix with the modified HPE matrix under the reference illuminant.

Lightness, J , is calculated from the achromatic signals of the stimulus, A , and white, A_w :

$$J = 100(A/A_w)^{c_z}. \quad (33)$$

Note 7: for A_w , Li and Luo²¹ showed that it is non-negative. However, for A , as noted in note 6 above, with the original CIECAM02 model, A may be negative; hence there is a problem for computing the lightness J . With the new version, however, as noted in note 6, A is non-negative; therefore, there is no problem with computing lightness J as long as the chromaticity coordinates of the input tristimulus values X , Y , Z are located inside or on the boundary of the region Ω_{CMF} .

Compute Q or brightness:

$$Q = (4/c) \cdot \sqrt{J/100} \cdot (A_w + 4) \cdot F_L^{0.25}. \quad (34)$$

Compute the eccentricity factor e_t and a temporary quantity, t , which are used for computing chroma C :

$$e_t = 1/4 \left[\cos \left(h \frac{\pi}{180} + 2 \right) + 3.8 \right] \quad (35)$$

$$t = \frac{(50000/13)N_c N_{cb} e_t (a^2 + b^2)^{1/2}}{R'_a + G'_a + (21/20)B'_a}. \quad (36)$$

Note 8: with the original CIECAM02 model, the denominator for computing the value of t may be zero,¹⁶ thus it causes unexpected mathematical failure for the CIECAM02 model. With the new version, however, the denominator is greater than 0.3 if the chromaticity coordinates of the input tristimulus values X , Y , Z are located inside or on the boundary of the region Ω_{CMF} .

Calculate chroma, C :

$$C = t^{0.9} \sqrt{J/100} (1.64 - 0.29^n)^{0.73}. \quad (37)$$

Calculate colorfulness, M :

$$M = CF_L^{0.25}. \quad (38)$$

Calculate saturation, s :

$$s = 100 \sqrt{M/Q}. \quad (39)$$

Performance of the New Version of the CIECAM02

Firstly, the corresponding visual data sets²⁵ were used to test the performance of the CAT02 matrix with the original matrix (Eq. (11)) and the (modified) HPE matrix (Eq. (12)). This set of data has 21 sub-datasets. All were used for deriving the CAT02.^{28,2} The average CIELAB color difference between the predicted and visual results is used as a performance measure. The results for each dataset are listed in Table II, including the reference and test illuminants, number of samples and the performance of the original and modified CAT02 matrix in terms of CIELAB color difference units. The last row lists the overall average color differences. It can be seen that the original CAT02 matrix performs better than the CAT02 with the (modified) HPE matrix for a majority of the datasets (17 out of 21), as might be expected. The original CAT02 matrix has an overall weighted mean CIELAB color difference of 5.48; on the other hand, the CAT02 with the (modified) HPE matrix has an overall weighted mean CIELAB color difference of 6.77. The CAT02 with the (modified) HPE matrix does not perform well on the following datasets: LUTCHI (D65/WF), Breneman (4), Breneman (8) and Breneman (9). On the other hand it performs slightly better than the original CAT02 matrix on the datasets LUTCHI (D65/D50), Breneman (6), Breneman (11) and Breneman (12). In the development of chromatic adaptation transforms, the three corresponding color datasets Lam,²⁹ CSAJ³⁰ and Helson et al.³¹ between D65 and A have been considered to be the most important because of the reliability of the experimental techniques used, the larger number of samples and observers used and the two most popular sources (D65 and A) used in the surface color industries. It can be seen that the CAT02 with the (modified) HPE matrix performs about 1.8, 1.5 and 1.2 CIELAB color difference units worse than the original CAT02 matrix on the Lam, CSAJ and Helson et al. datasets respectively. Overall, the CAT02 with the (modified) HPE matrix performs about 1.3 CIELAB color difference units worse than the original CAT02 matrix.

These three datasets were further analyzed. Figure 1 shows a plot of the color shifts of the visual results, the prediction from the original CAT02 matrix and HPE CAT02 matrix represented by the solid, dotted and dashed lines, respectively. The three datasets are also plotted in different colors, i.e., blue, red and black for the Lam, CSAJ and

Table II. Average CIELAB color difference values under each data set for the original CAT02 and the CAT02 with the HPE matrix.

Data set	Reference illuminant	Test illuminant	No. of samples	Original CAT02	CAT02 with M_{HPE}
CSAJ	D65	A	87	3.99	<u>5.48</u>
Kuo	D65	A	40	4.97	<u>6.81</u>
Kuo	D65	TL84	41	3.55	<u>4.90</u>
Lam	D65	A	58	4.42	<u>6.21</u>
Helson	C	A	59	4.93	6.04
LUTCHI	D65	A	43	5.65	6.13
LUTCHI	D65	D50	44	6.62	6.35
LUTCHI	D65	WF	41	6.96	<u>9.89</u>
Breneman (1)	D65	A	12	7.74	8.02
Breneman (2)	D55	Projector	12	5.11	5.53
Breneman (3)	D55	Projector	12	8.25	11.08
Breneman (4)	D65	A	11	9.82	13.44
Breneman (6)	D65	A	12	7.47	7.39
Breneman (8)	D65	A	12	8.82	12.51
Breneman (9)	D65	A	12	14.21	18.94
Breneman (11)	Green	D55	12	6.62	4.63
Breneman (12)	Green	D55	12	7.16	6.02
Braun & Fairchild (1)	D65	D65	17	3.15	3.68
Braun & Fairchild (2)	D65	D65	16	5.07	5.31
Braun & Fairchild (3)	D65	D93	17	3.68	<u>5.65</u>
Braun & Fairchild (4)	D65	A	14	3.77	4.10
Weighted Mean				5.48	6.77

Helson datasets respectively. Detailed inspection shows that the original CAT02 matrix almost outperformed the HPE CAT02 matrix for all colors, i.e., the end point of the dotted vector is closer to that of the solid vector than to that of the dashed vector. This effect could be significant.

Next, the color appearance data sets²⁷ were used to test the original CIECAM02 model against the new version. To assess the fit to the experimental data, the value of CV (coefficient of variation) was used. Note that the CV value has been used to measure the performance of various color appearance models³² and CIECAM02.³³ Let V_i and P_i , $i = 1, 2, \dots, n$, be the visual and model predicted results. The CV value measures the closeness of the model prediction to the visual results, as defined by

$$CV = 100 \left[\frac{1}{n} \sum_{i=1}^n (V_i - P_i)^2 \right]^{1/2} / \left[\frac{1}{n} \sum_{i=1}^n V_i \right]. \quad (40)$$

The lower the CV value, the better the performance of the model. For example, $CV = 20$ means that there is a 20% difference between the visual results and the model prediction. All the results are listed in Table III. It can be seen from Table III that the new version performs worse than the original CIECAM02 model, as expected. The differences, however, are small (0.18, 0.28 and 0.12 CV units worse for lightness, colorfulness and hue composition respectively).

CONCLUSIONS

In this article, a modification to the CIECAM02 model with a modified HPE matrix has been presented, including both the forward and reverse models. Additionally, the nonlinear luminance adaptation function was extended. The modified CIECAM02 model is simpler and overcomes the computational inconsistency existing with the present CIECAM02 model as well as the instability associated with the inverse model. The performance of the proposed modification was tested using the color appearance datasets based on the magnitude estimation method. It was found that the proposed modification performed 0.3 CV units worse than the CIECAM02 for lightness, colorfulness and hue composition correlate attributes. Replacement of the CAT02 matrix with the (modified) HPE matrix was tested using the color appearance datasets based on corresponding colors. The modified version performed about 1.3 CIELAB color difference units worse than the original CAT02 in 17 out of 21 data sets. Furthermore, comparing the most important three datasets between A and D65 illuminants, the original CAT02 matrix significantly outperformed the HPE CAT02 matrix for almost all corresponding colors.

ACKNOWLEDGMENT

This work was supported by the Natural Science Foundation of China with Grant Number 61178053. The authors thank the reviewers for their suggestions and criticisms, and Mike

Table III. Performance of the CIECAM02 model and the revised version in terms of lightness, colorfulness and hue composition CV values when predicting all color appearance visual datasets.

Groups	Lightness		Colorfulness		Hue composition	
	Original CIECAM02	New CIECAM02	Original CIECAM02	New CIECAM02	Original CIECAM02	New CIECAM02
RHL	10.64	10.94	17.79	17.94	6.88	6.92
RLL	11.35	11.70	18.56	18.84	7.08	7.16
RVL	13.31	13.46	18.39	18.92	6.53	6.52
RTE	14.85	14.76	23.67	24.76	7.07	7.14
CRT	11.65	11.69	19.61	19.51	6.74	7.59
M35	19.33	19.97	16.06	16.24	7.23	7.49
LTX	16.53	16.59	14.20	14.44	5.81	5.60
JUA	14.24	14.23	20.34	20.25	7.65	7.49
Mean	13.99	14.17	18.58	18.86	6.87	6.99

Pointer for reading and correcting the manuscript, which improved the quality of the article.

Appendix. Inverse Model for the Modified CIECAM02

Input: J or Q ; C , M , or s ; H or h

Output: X , Y , Z (under test illuminant X_w , Y_w , Z_w)

The illuminants, viewing surrounds, and background parameters are the same as those given in the forward mode.

Step 0: Calculate viewing and adaptation parameters

Compute all k , F_L , n , z , $N_{bb} = N_{bc}$, R_w , G_w , B_w , D , Λ_R , Λ_G , Λ_B , R_{wc} , G_{wc} , B_{wc} , R'_{aw} , G'_{aw} , B'_{aw} and A_w using the same formulas as found in Step 0 of the forward model. They are needed in the following steps. Note that all data computed in this step can be used for all samples (for example all pixels of an image) under the defined viewing conditions. Hence they are computed only once. The following computing steps are sample/pixel dependent.

Step 1: Obtain J , C and h from H , Q , M , s

Entering of the data can be in different combinations of perceived correlates, i.e., J or Q ; C , M or s ; and H or h . Hence the following are needed to derive the missing correlates J , C and h .

Step 1-1: Compute J from Q (if starting from Q)

$$J = 6.25 \cdot \left[\frac{c \cdot Q}{(A_w + 4) \cdot F_L^{0.25}} \right]^2.$$

Step 1-2: Calculate C from M or s

$$C = \frac{M}{F_L^{0.25}} \quad (\text{if starting from } M)$$

$$Q = \left(\frac{4}{c} \right) \cdot \left(\frac{J}{100} \right)^{0.5} \cdot (A_w + 4.0) \cdot F_L^{0.25}$$

$$\text{and } C = \left(\frac{s}{100} \right)^2 \cdot \left(\frac{Q}{F_L^{0.25}} \right) \quad (\text{if starting from } s)$$

Step 1-3: Calculate h from H (if starting from H)

The correlate of hue (h) can be computed by using the data in Table I in the forward mode.

Choose a proper i ($i = 1, 2, 3$ or 4) so that $H_i \leq H < H_{i+1}$.

$$h' = \frac{(H - H_i) \cdot (e_{i+1}h_i - e_i \cdot h_{i+1}) - 100 \cdot h_i \cdot e_{i+1}}{(H - H_i) \cdot (e_{i+1} - e_i) - 100 \cdot e_{i+1}}.$$

Set $h = h' - 360$ if $h' > 360$, otherwise $h = h'$.

Step 2: Calculate t , e_t , p_1 , p_2 and p_3

$$t = \left[\frac{C}{\sqrt{\frac{J}{100}} \cdot (1.64 - 0.29n)^{0.73}} \right]^{0.9}$$

$$e_t = \frac{1}{4} \cdot \left[\cos \left(h \cdot \frac{\pi}{180} + 2 \right) + 3.8 \right]$$

$$A = A_w \cdot \left(\frac{J}{100} \right)^{\frac{1}{c \cdot z}}$$

$$p_1 = \left(\frac{50000}{13} \cdot N_c \cdot N_{cb} \right) \cdot e_t \cdot \left(\frac{1}{t} \right), \quad \text{if } t \neq 0$$

$$p_2 = \frac{A}{N_{bb}} + 0.305$$

$$p_3 = \frac{21}{20}.$$

Step 3: Calculate a and b

If $t = 0$, then $a = b = 0$ and **go to Step 4** (be sure to transform h from degrees to radians before calculating $\sin(h)$ and $\cos(h)$)

If $|\sin(h)| \geq |\cos(h)|$ then

$$p_4 = \frac{p_1}{\sin(h)}$$

$$b = \frac{p_2 \cdot (2 + p_3) \cdot \left(\frac{460}{1403} \right)}{p_4 + (2 + p_3) \cdot \left(\frac{220}{1403} \right) \cdot \left(\frac{\cos(h)}{\sin(h)} \right) - \left(\frac{27}{1403} \right) + p_3 \cdot \left(\frac{6300}{1403} \right)}$$

$$a = b \cdot \left(\frac{\cos(h)}{\sin(h)} \right).$$

If $|\cos(h)| > |\sin(h)|$, then

$$p_5 = \frac{p_1}{\cos(h)}$$

$$a = \frac{p_2 \cdot (2+p_3) \cdot \left(\frac{460}{1403}\right)}{p_5 + (2+p_3) \cdot \left(\frac{220}{1403}\right) - \left[\left(\frac{27}{1403}\right) - p_3 \cdot \left(\frac{6300}{1403}\right)\right] \cdot \left(\frac{\sin(h)}{\cos(h)}\right)}$$

$$b = a \cdot \left(\frac{\sin(h)}{\cos(h)} \right).$$

Step 4: Calculate R'_a , G'_a and B'_a

$$R'_a = \frac{460}{1403} \cdot p_2 + \frac{451}{1403} \cdot a + \frac{288}{1403} \cdot b$$

$$G'_a = \frac{460}{1403} \cdot p_2 - \frac{891}{1403} \cdot a - \frac{261}{1403} \cdot b$$

$$B'_a = \frac{460}{1403} \cdot p_2 - \frac{220}{1403} \cdot a - \frac{6300}{1403} \cdot b.$$

Step 5: Calculate R_c , G_c and B_c

$$R_c = \begin{cases} \frac{(R'_a - f(q_L))}{df(q_L)/dq} + q_L & \text{if } R'_a \leq f(q_L) \\ \frac{100}{F_L} \cdot \left[\frac{27 \cdot 13 \cdot (R'_a - 0.1)}{400 - (R'_a - 0.1)} \right]^{\frac{1}{0.42}} & \text{if } f(q_L) < R'_a < f(q_U) \\ \frac{(R'_a - f(q_U))}{df(q_U)/dq} + q_U & \text{if } R'_a \geq f(q_U). \end{cases}$$

Similarly compute G_c and B_c from G'_a and B'_a .

Step 6: Calculate R , G and B from R_c , G_c and B_c

$$\begin{pmatrix} R \\ G \\ B \end{pmatrix} = \begin{pmatrix} R_c / \Lambda_R \\ G_c / \Lambda_G \\ B_c / \Lambda_B \end{pmatrix}.$$

Step 7: Calculate X , Y and Z using

$$\begin{pmatrix} X \\ Y \\ Z \end{pmatrix} = M_{\text{HPE}}^{-1} \cdot \begin{pmatrix} R \\ G \\ B \end{pmatrix}.$$

REFERENCES

- Commission Internationale de l'Éclairage. CIE TC8-01 Technical Report. A color appearance model for color management systems: CIECAM02. CIE Pub. 159: 2004.
- N. Moroney, M. D. Fairchild, R. W. G. Hunt, C. J. Li, M. R. Luo, and T. Newman, "The CIECAM02 colour appearance models," *Proc. IS&T/SID Tenth Color Imaging Conf.* (IS&T, Springfield, VA, 2002), pp. 23–27.
- Seo Young Choi, M. Ronnier Luo, Michael R. Pointer, and Peter A. Rhodes, "Investigation of large display color image appearance I: important factors affecting perceived quality," *J. Imaging Sci. Technol.* **52**, 40904-1–40904-11 (2008).
- Seo Young Choi, M. Ronnier Luo, Michael R. Pointer, and Peter A. Rhodes, "Investigation of large display color image appearance II: the influence of surround conditions," *J. Imaging Sci. Technol.* **52**, 40905-1–40905-9 (2008).
- Seo Young Choi, M. Ronnier Luo, Michael R. Pointer, and Peter A. Rhodes, "Investigation of large display color image appearance—III: modeling image naturalness," *J. Imaging Sci. Technol.* **53**, 31104-1–31104-12 (2009).
- Changjun Li, M. Ronnier Luo, and Guihua Cui, "Colour-difference evaluation using colour appearance models," *Proc. IS&T/SID Eleventh Color Imaging Conf.* (IS&T, Springfield, VA, 2003), pp. 127–131.
- M. R. Luo, G. H. Cui, and C. J. Li, "Uniform color spaces based on CIECAM02 color appearance model," *Color Res. Appl.* **31**, 320 (2006).
- Ingeborg Tastl, Miheer Bhachech, Nathan Moroney, and Jack Holm, "ICC color management and CIECAM02," *Proc. IS&T/SID Thirteenth Color Imaging Conf.* (IS&T, Springfield, VA, 2005), pp. 217–223.
- Kuo Chunhui, Zeise Eric, and Lai Di, "Robust CIECAM02 implementation and numerical experiment within an international color consortium workflow," *J. Imaging Sci. Technol.* **52**, (2008)20603-1–20603-6(6).
- C. H. Kuo, E. Zeise, and D. Lai, "Robust CIECAM02 implementation and numerical experiment within an ICC workflow," *Proc. IS&T/SID Fourteenth Color Imaging Conf.* (IS&T, Springfield, VA, 2006), pp. 215–219.
- M. H. Brill, "Irregularity in CIECAM02 and its avoidance," *Color Res. Appl.* **31**, 142–145 (2006).
- S. Süsstrunk and M. H. Brill, "The nesting instinct: repairing non-nested gamuts in CIECAM02," *Proc. IS&T/SID Fourteenth Color Imaging Conf.* (IS&T, Springfield, VA, 2006).
- Michael H. Brill and Sabine Süsstrunk, "Repairing Gamut Problems in CIECAM02: A Progress Report," *Color Res. Appl.* **33**, 424–426 (2008).
- C. J. Li, E. Perales, M. R. Luo, and F. Martínez-Verdú, "Mathematical approach for predicting non-negative tristimulus values using the CAT02 chromatic adaptation transform," *Color Res. Appl.* **27**, 255–260 (2012).
- R. Guay and M. Shaw, "Dealing with imaginary color encodings in CIECAM02 in an ICC work flow," *Proc. IS&T/SID Thirteenth Color Imaging Conf.* (IS&T, Springfield, VA, 2005), p. 318.
- G. W. Gill, "A solution to CIECAM02 numerical and range issues," *Proc. IS&T/SID Sixteenth Color Imaging Conf.* (IS&T, Springfield, VA, 2010), pp. 327–331.
- C. J. Li, E. Chorro-Calderon, M. R. Luo, and M. R. Pointer, "Recent progress with extensions to CIECAM02," *Proc. IS&T/SID Seventeenth Color Imaging Conf.* (IS&T, Springfield, VA, 2009), pp. 69–74.
- M. H. Brill and M. Mahy, "Visualization of mathematical inconsistencies in CIECAM02," *Color Res. Appl.* (2012)Article first published online: DOI: 10.1002/col.20744.
- C. J. Li, M. R. Luo, and P. L. Sun, "A New Version of CIECAM02 with the HPE Primaries," *Proc. IS&T CGIV 2010/MCS'10 5th European Conf. on Colour in Graphics, Imaging, and Vision* (IS&T, Springfield, VA, 2010), pp. 151–154.
- C. J. Li, M. R. Luo, and Z. F. Wang, "Different Matrices for CIECAM02," *Color Res. Appl.* (2012)(in press). First published online: DOI: 10.1002/col.21765.
- C. J. Li and M. R. Luo, "Testing the robustness of CIECAM02," *Color Res. Appl.* **30**, 99–106 (2005).
- Mark D. Fairchild, "A revision of CIECAM97s for practical applications," *Color Res. Appl.* **26**, 418–427 (2001).
- Mark D. Fairchild, *Color Appearance Models*, second edition (John Wiley & Sons, Ltd., 2005).
- S. Süsstrunk, J. Holm, and G. D. Finlayson, "Chromatic adaptation performance of different RGB sensors," *Proc. SPIE* **4300**, (2001).
- Li Changjun, M. R. Luo, B. Rigg, and R. W. G. Hunt, "CMC 2000 Chromatic Adaptation Transform: CMCCAT2000," *Color Res. Appl.* **27**, 49–58 (2002).
- M. R. Luo and R. W. G. Hunt, "A chromatic adaptation transform and a colour inconstancy index," *Color Res. Appl.* **23**, 154–158 (1998).
- M. R. Luo, A. A. Clarke, P. A. Rhodes, A. Schappo, S. A. R. Scribner, and C. J. Tait, "Quantifying colour appearance: Part I –LUTCHI colour appearance data," *Color Res. Appl.* **16**, 166–180 (1991).
- R. W. G. Hunt, C. J. Li, M. Y. Juan, and M. R. Luo, "Further improvements to CIECAM97s," *Color Res. Appl.* **27**, 164–170 (2002).
- K. M. Lam, "Metamerism and colour constancy," Ph.D. thesis (University of Bradford, UK, 1985).
- L. Mori, H. Sobagaki, H. Komatsubara, and K. Ikeda, "Field trials on CIE chromatic adaptation formula," *Proc. CIE 22th session* (1991) pp. 55–58.
- H. Helson, D. B. Judd, and M. H. Warren, "Object color changes from daylight to incandescent filament illumination," *Illum. Eng.* **47**, 221–233 (1952).
- M. R. Luo and R. W. G. Hunt, "Testing colour appearance models using corresponding colour and magnitude-estimation data sets," *Color Res. Appl.* **23**, 147–153 (1998).
- C. J. Li, M. R. Luo, R. W. G. Hunt, N. Moroney, M. D. Fairchild, and T. Newman, *Proc. IS&T/SID Tenth Color Imaging Conf.* (IS&T, Springfield, VA, 2002), pp. 28–32.